

Electro-Oxidation of Formic Acid on PdIr/C-Sb₂O₅.SnO₂ Electrocatalysts Prepared by Borohydride Reduction

J. Nandenha, R.F.B. De Souza, M.H.M.T. Assumpção, E.V. Spinacé, A.O. Neto*

Instituto de Pesquisas Energéticas e Nucleares – IPEN-CNEN/SP, Av. Prof. Lineu Prestes, 2242, Cidade Universitária, 05508-900 São Paulo, SP, Brazil

*E-mail: aolivei@ipen.br

Received: 22 April 2013 / Accepted: 7 June 2013 / Published: 1 July 2013

PdIr/C-Sb₂O₅.SnO₂ electrocatalysts with different atomic ratio (90:10, 70:30 and 50:50) were prepared by borohydride reduction method using a water/2-propanol mixture as solvent, Pd(NO₃)₂.2H₂O and IrCl₃.3H₂O as metal sources, a physical mixture of 85% Vulcan Carbon XC72 and 15% Sb₂O₅.SnO₂ (ATO) as support and NaBH₄ as reducing agent. The obtained materials were characterized by X-ray diffraction (XRD) and transmission electron microscopy (TEM), while the catalytic activity for formic acidic electro-oxidation was investigated by cyclic voltammetry and chronoamperometry. X-ray diffractograms of PdIr/C-Sb₂O₅.SnO₂ electrocatalysts showed the presence of Pd(fcc) phase, carbon and ATO phases. These electrocatalysts did not show peaks related to Ir, however the presence of Ir oxides in small amounts and amorphous forms cannot be discarded. TEM micrographs and histograms of the particle size distributions showed that the nanoparticles of PdIr electrocatalysts were not well dispersed on the support and some agglomerates were present. The electrochemical studies showed that PdIr/C-Sb₂O₅.SnO₂ (90:10) and PdIr/C-Sb₂O₅.SnO₂ (50:50) had superior performance for formic acid electro-oxidation at 25°C compared to Pd/C-Sb₂O₅.SnO₂. These results indicated that addition of Ir to Pd could favor the electro-oxidation of formic acid, therefore this effect could be attributed to bifunctional mechanism associated to electronic effect.

Keywords: PdIr/C-Sb₂O₅.SnO₂ electrocatalysts; formic acid oxidation, borohydride reduction process

1. INTRODUCTION

Fuel cell has been considered as attractive option for power generation due to their high efficiency and little or no pollution [1]. Among various types of fuel cells, direct liquid fuel cell has been considered very attractive as power sources for stationary, mobile and portable applications [2], while Methanol has been the fuel most studied for polymer electrolyte membrane fuel cells (DMFC)

due to their low cost, low pollutant emissions and high theoretical energy density. Nevertheless the use of methanol is not safe because it is a toxic, evaporable and burnable compound [3].

Therefore, formic acid has been proposed as an alternative to methanol, because it exhibits a smaller crossover flux through Nafion[®] than methanol, allowing the use of highly concentrated fuel solutions. Moreover, formic acid is also not inflammable and its storage and transportation are safe [4].

For the formic acid electro-oxidation, Pt-based and Pd-based catalysts have been most frequently employed. On Pt based electrocatalysts the formic acid oxidation has been mainly via an indirect path, where the electrocatalyst is easily poisoned by the adsorbed CO at low potential [5, 6]. Pd electrocatalysts has been able to catalyze formic acid oxidation and it is less inclined to CO poisoning and deactivation, in comparison with Pt, because the electro-oxidation of formic acid on these materials is mainly through the direct pathway. Nevertheless, the catalytic activity and durability of Pd catalysts still need to be substantially improved, consequently, the addition of co-catalysts to palladium is yet necessary [6, 7].

Considering Pd binary electrocatalysts, it has been suggested that the second atom can increase the adsorption ability of the active oxygen and then the oxidation rate of formic acid. Another suggestion is that the co-catalysts could also prevent from the formation of strongly adsorbed CO [8].

Wang *et al.* [8] showed that the electrocatalytic activity of Pd-Ir/C was better than only Pd/C electrocatalyst, although Ir has no electrocatalytic activity for the oxidation of formic acid. These authors concluded that Ir could promote the oxidation of formic acid at Pd through the direct pathway, because Ir can decrease the adsorption strength of CO on Pd. The use of iridium is interesting for direct liquid fuel cell, since iridium oxide shows an excellent corrosion resistance in acidic medium, good electrical conductivity, and high electrocatalytic activity towards oxygen evolution.

Considering also the addition of oxides into carbon as support, it can enhance the catalytic activity for small organic molecule electro-oxidation through synergetic interaction between oxides, the carbon and noble metals. Among those, Sb₂O₅.SnO₂ (ATO) exhibit a number of characteristics that make them interesting for catalytic studies due to enhancement of electrical conductivity compared with others oxides. The presence of ATO oxides could also be beneficial to the oxidation of some poisoning intermediates adsorbed on palladium (bifunctional mechanism) [5, 9, 10].

In this context, the aim of this work was prepare PdIr/C-Sb₂O₅.SnO₂ electrocatalysts by borohydride reduction and test these materials for formic acid electro-oxidation in acidic medium by cyclic voltammetry and chronoamperometry.

2. EXPERIMENTAL

PdIr/C-Sb₂O₅.SnO₂ (20 wt.% of metals loading, with Pd:Ir atomic ratio of 90:10, 70:30 and 50:50) were prepared by borohydride reduction method using a water/2-propanol mixture as solvent (3:1), Pd(NO₃)₂.2H₂O and IrCl₃.3H₂O as metal sources, a physical mixture of 85% Vulcan Carbon XC72 and 15% Sb₂O₅.SnO₂ (ATO) as support and NaBH₄ as reducing agent. The preparation of electrocatalysts was realized in accordance with reference 9.

X-ray diffraction (XRD) analyses were performed using a Rigaku diffractometer model Miniflex II using Cu K α radiation source ($\lambda = 0.15406$ nm). The diffractograms were recorded from $2\theta = 20^\circ$ to 90° with a step size of 0.05° and a scan time of 2s per step, while transmission electron microscopy (TEM) was carried using a JEOL JEM-2100 electron microscope operated at 200 kV. The mean nanoparticle sizes were determined by counting more than 200 particles from different regions of each sample.

The cyclic voltammetry and chronoamperometry measurements were carried out at room temperature using a Microquimica potentiostat. These study were performed using a working electrodes (geometric area of 0.3 cm^2 with a depth of 0.3 mm) prepared using the thin porous coating technique [11]. The reference electrode was a reversible hydrogen electrode (RHE) and the counter electrode was a Pt plate. The electrochemical measurements were realized in presence of 0.5 molL^{-1} H_2SO_4 or 1.0 mol L^{-1} of formic acid + 0.5 mol L^{-1} H_2SO_4 solutions saturated with N_2 .

3. RESULTS AND DISCUSSION

The X-ray diffractograms of PdIr/C-Sb $_2$ O $_5$.SnO $_2$ electrocatalysts prepared with different Pd:Ir atomic ratio are shown in Fig. 1. All diffractograms showed a broad peak at about 25° associated with the Vulcan XC72 support, four peaks at approximately $2\theta = 40^\circ, 47^\circ, 67^\circ$ and 82° , which are associated with the fcc structure characteristic of Pd (JCPDF # 89-4897) or Pd alloys and peaks at about $2\theta = 27^\circ, 34^\circ, 38^\circ, 52^\circ, 55^\circ, 62^\circ, 65^\circ, 66^\circ$, which were also characteristic of ATO used as support.

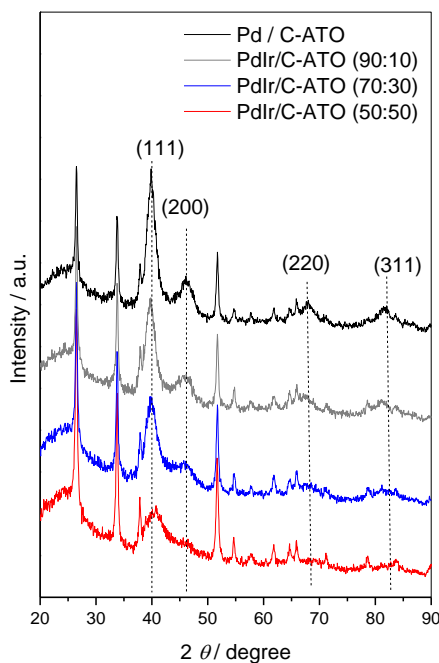
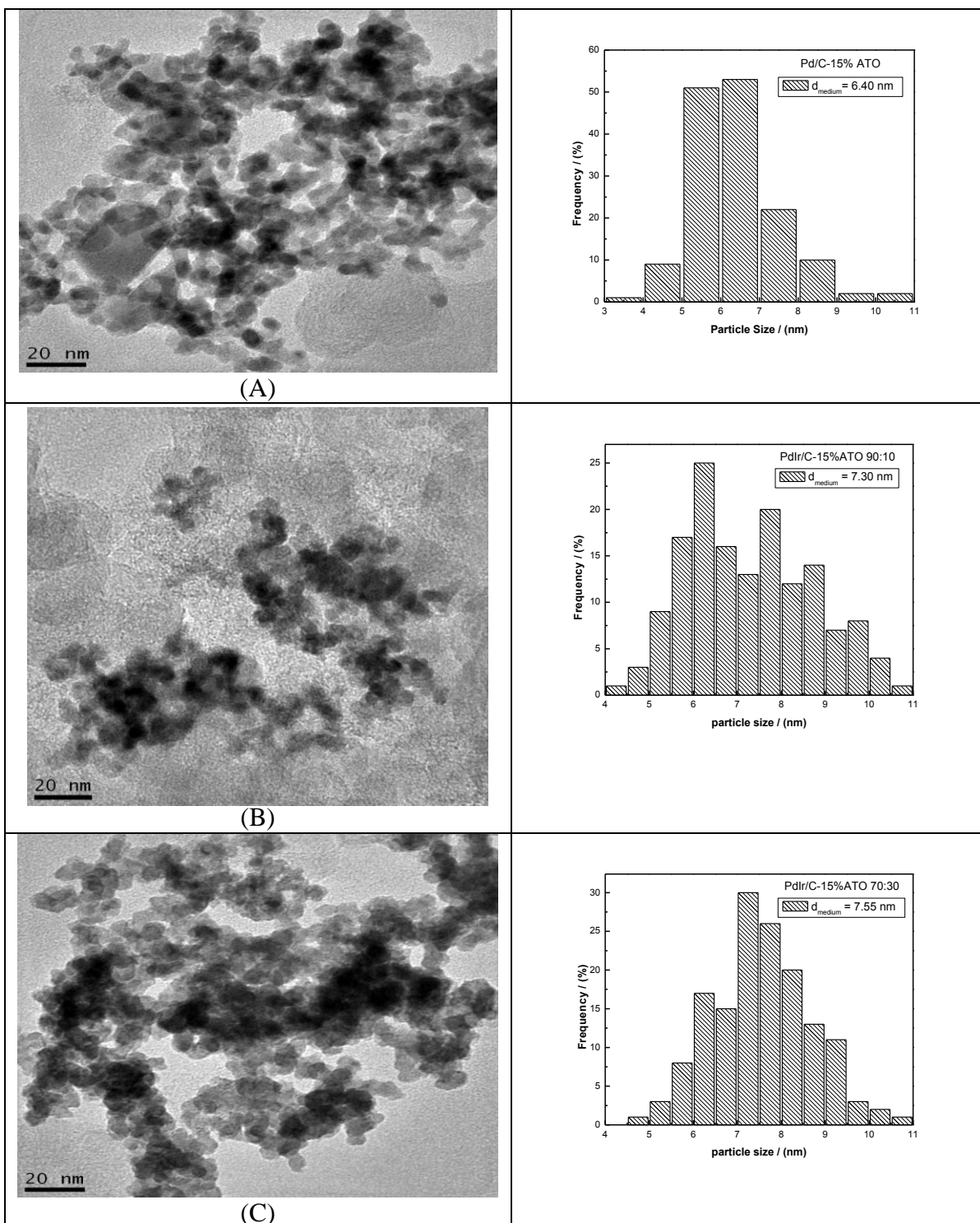


Figure 1. X-ray diffractograms of the Pd/C-Sb $_2$ O $_5$.SnO $_2$ and PdIr/C-Sb $_2$ O $_5$.SnO $_2$ electrocatalysts.

For all PdIr/C-Sb₂O₅.SnO₂ no peaks related to Ir were observed, however the presence of Ir oxides in small amounts and amorphous forms cannot be discarded. PdIr/C-Sb₂O₅.SnO₂ (50:50) electrocatalyst showed a shift to higher angles of the peak associated to the (220) plane compared to Pd/C-Sb₂O₅.SnO₂ indicating the insertion of Ir in the Pd structure. Also it was found that the peaks of Pd particles in the Pd/C-Sb₂O₅.SnO₂ electrocatalysts are higher and sharper than that of the PdIr/C-Sb₂O₅.SnO₂ (50:50), consequently the average size and crystallinity of PdIr/C-Sb₂O₅.SnO₂ (50:50) is smaller than that of the Pd/C-Sb₂O₅.SnO₂.



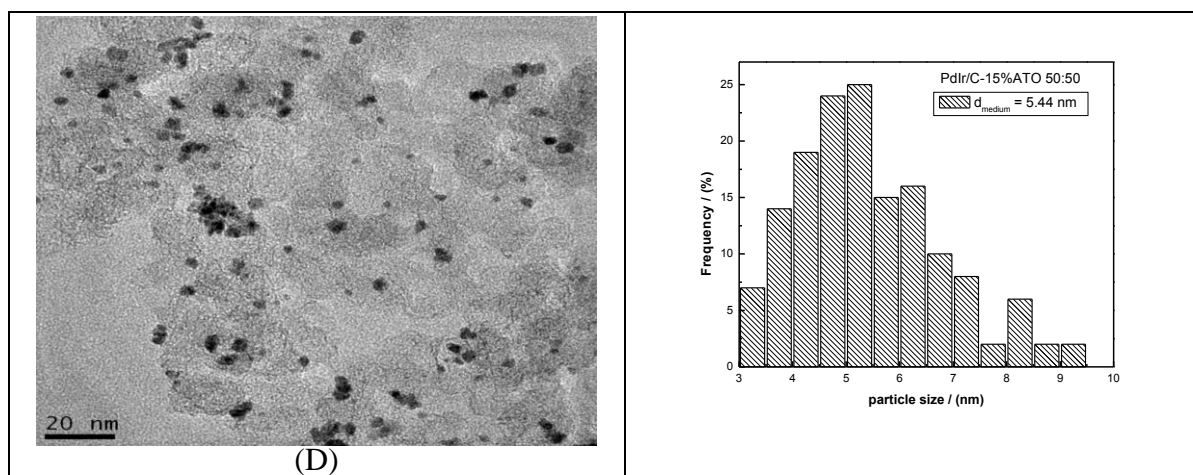


Figure 2. TEM micrograph and a histogram of (2a) Pd/C-Sb₂O₅.SnO₂, (2b) PdIr/C-Sb₂O₅.SnO₂ (90:10), (2c) PdIr/C-Sb₂O₅.SnO₂ (70:30) and (2d) PdIr/C-Sb₂O₅.SnO₂ (50:50) electrocatalyst with the mean diameter and particle distribution.

Therefore, the presence of Ir could prevent from the aggregation of the particles as an observed by Wang *et al.* [8].

TEM micrographs and histograms of the particle size distributions of Pd/C-Sb₂O₅.SnO₂ and PdIr/C-Sb₂O₅.SnO₂ electrocatalysts are shown in Figure 2.

Pd/C-Sb₂O₅.SnO₂, PdIr/C-Sb₂O₅.SnO₂ (90:10) and PdIr/C-Sb₂O₅.SnO₂ (70:30) showed that the nanoparticles were not well dispersed on the support and some agglomerates were present, while PdIr/C-Sb₂O₅.SnO₂ (50:50) electrocatalyst showed the nanoparticles well dispersed on the support. The mean particle sizes of Pd/C-Sb₂O₅.SnO₂, PdIr/C-Sb₂O₅.SnO₂ (90:10), PdIr/C-Sb₂O₅.SnO₂ (70:30) and PdIr/C-Sb₂O₅.SnO₂ (50:50) electrocatalysts were 6.4 nm, 7.3 nm, 7.6 nm and 5.4 nm, respectively. The addition of 50% Ir to Pd/C-Sb₂O₅.SnO₂ resulted in a decrease of mean particle size indicating that higher concentration of Ir could prevent an aggregation of the particles. This result is in accordance with X-ray diffractogram study.

According to Marinšek *et al.* [12] catalytic activity of Pd-based catalysts depends strongly on the size, shape and size distribution of the metal particles and generally, the smaller the Pd-particles enhanced the electro-activity for formic acid oxidation. In terms of beneficial particle size effects, 5-7 nm Pd-nanoparticles were reported to be the most favorable for formic acid electro-oxidation [12, 13].

The cyclic voltammograms of Pd/C-Sb₂O₅.SnO₂, PdIr/C-Sb₂O₅.SnO₂ (90:10), PdIr/C-Sb₂O₅.SnO₂ (70:30) and PdIr/C-Sb₂O₅.SnO₂ (50:50) electrocatalysts in presence of 0.5 mol L⁻¹ of H₂SO₄ solution are shown in Figure 3.

The voltammograms of PdIr/C-Sb₂O₅.SnO₂ (70:30) and PdIr/C-Sb₂O₅.SnO₂ (50:50) electrocatalysts do not display a well-defined hydrogen oxidation region (0.0–0.4V versus RHE) in comparison with Pd/C-Sb₂O₅.SnO₂, PdIr/C-Sb₂O₅.SnO₂ (90:10). The current densities of all PdIr/C-Sb₂O₅.SnO₂ in the double layer region (between 0.45 and 0.65V versus RHE) are larger than those on Pd/C-Sb₂O₅.SnO₂, this behavior is characteristic of binary and ternary electrocatalysts [14].

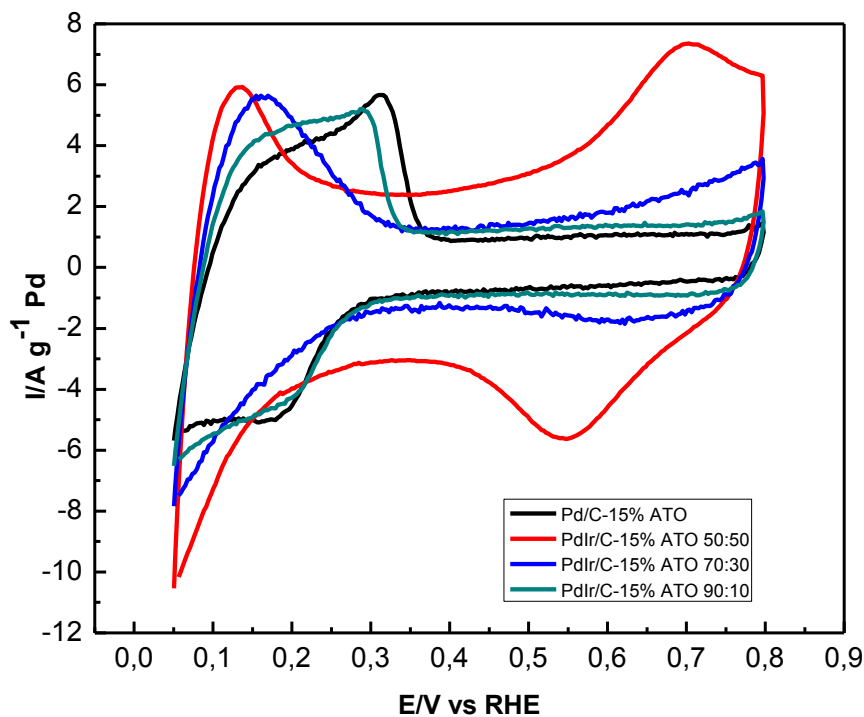


Figure 3. Cyclic voltammograms of Pd/C-Sb₂O₅.SnO₂ and PdIr/C-Sb₂O₅.SnO₂ electrocatalysts in 0.5 mol L⁻¹ H₂SO₄ with a sweep rate of 10 mV s⁻¹.

The charge–discharge current of the double layer at the PdIr/C-Sb₂O₅.SnO₂ (50:50) electrocatalyst was largest among all electrocatalysts, this behavior could be attributed to smallest average size of the metal particles and the largest surface area. The voltammograms of PdIr/C-Sb₂O₅.SnO₂ (70:30) PdIr/C-Sb₂O₅.SnO₂ (50:50) electrocatalysts are also suppressed in comparison with Pd/C-Sb₂O₅.SnO₂ indicating partial coverage of Pd by Ir.

PdIr/C-Sb₂O₅.SnO₂ (50:50) and PdIr/C-Sb₂O₅.SnO₂ (70:30) electrocatalysts also showed the clear shifts of the peak positions for the hydrogen adsorption-desorption in comparison with others electrocatalysts prepared, therefore this negative shift is an indication of the electronic modification of Pd atoms by the neighboring Ir atoms [12].

The presence of an oxidation process in potential (0.7V) could be related as Ir oxide species, where Juodkazis et al [15] has reported the existence of reversible metal-oxide layers for noble metals such as iridium, oxidized anodically in the range of potentials before O₂ evolution.

Fig. 4 shows the cyclic voltammograms of Pd/C-Sb₂O₅.SnO₂ and PdIr/C-Sb₂O₅.SnO₂ electrocatalysts prepared at 25°C in presence of 1.0 mol L⁻¹ formic acid in 0.5 mol L⁻¹ H₂SO₄. All PdIr/C-Sb₂O₅.SnO₂ electrocatalysts showed highest current values in all potential range in comparison with Pd/C-Sb₂O₅.SnO₂. PdIr/C-Sb₂O₅.SnO₂ (70:30) electrocatalyst showed a best performance in potential of 0.05 to 0.45 V, while that PdIr/C-Sb₂O₅.SnO₂ (50:50) showed higher currents values in comparison to PdIr/C-Sb₂O₅.SnO₂ (70:30) and PdIr/C-Sb₂O₅.SnO₂ (90:10) electrocatalysts for

potentials above of 0.45V. The high activity of PdIr/C-Sb₂O₅.SnO₂ (50:50) electrocatalysts could be attributed to smaller average sizes particle in comparison with others electrocatalysts prepared.

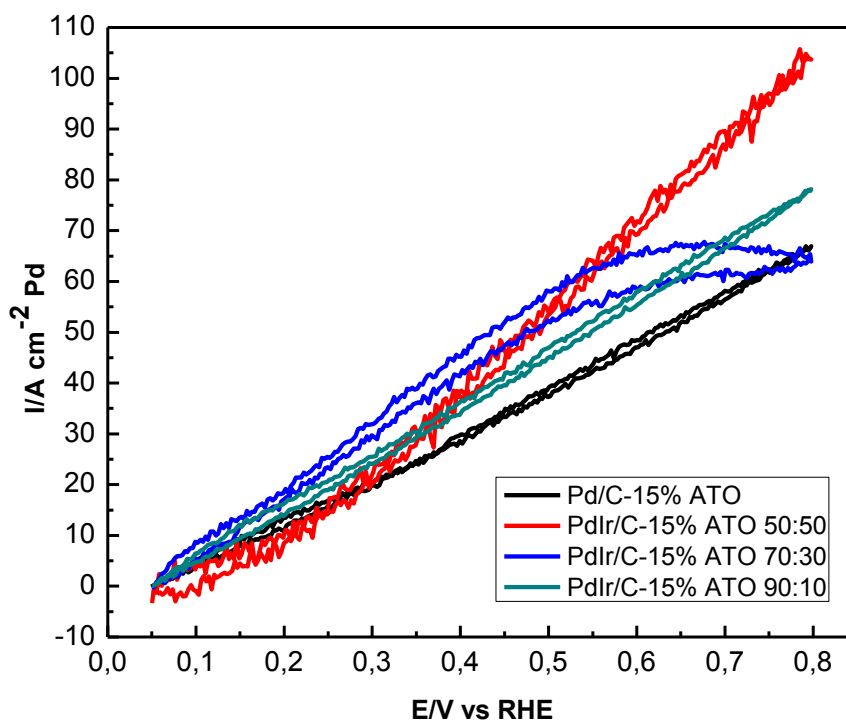


Figure 4. Cyclic voltammograms of the Pd/C-Sb₂O₅.SnO₂, PdIr/C-Sb₂O₅.SnO₂ (90:10), PdIr/C-Sb₂O₅.SnO₂ (70:30) and PdIr/C-Sb₂O₅.SnO₂ (50:50) electrocatalysts in 1 mol L⁻¹ formic acid solution in 0.5 mol L⁻¹ H₂SO₄ with a sweep rate of 10 mV s⁻¹ at 25°C.

The introduction of Ir leads to an increase in the electro-activity of the binary electrocatalysts (PdIr) compared to pure Pd. This effect could be also explained by the activation of interfacial water molecules at lower potentials than in the case of pure Pd due to the presence of preferential sites for OH_{ads} adsorption, where the presence of OH_{ads} species is necessary for the complete oxidation of poisoning intermediates adsorbed [14]. The electro-oxidation of formic acid on PdIr/C-Sb₂O₅.SnO₂ electrocatalysts could also occur in the direct pathway, where formic acid is directly oxidized to CO₂. In accordance, Wang et. al. [7] showed that the electrocatalytic activity of the PdIr/C (50:50) and PdIr/C (70:30) for the oxidation of formic acid was highest among all the electrocatalysts prepared.

Fig. 5 shows the current-time curves for formic acidic electro-oxidation for Pd/C-Sb₂O₅.SnO₂, PdIr/C-Sb₂O₅.SnO₂ (90:10), PdIr/C-Sb₂O₅.SnO₂ (70:30) and PdAu/C-Sb₂O₅.SnO₂ (50:50) electrocatalysts at 25°C in the potential of 0.5 V for 30 min.

All of the catalysts featured a pronounced current decay in the first 2 min due to the accumulation of poisonous intermediates, and the current values of PdIr/C-Sb₂O₅.SnO₂ (50:50), PdIr/C-Sb₂O₅.SnO₂ (90:10) and Pd/C-Sb₂O₅.SnO₂ decay slowed down at longer times, while that PdIr/C-Sb₂O₅.SnO₂ (70:30) electrocatalyst showed a decay sharply.

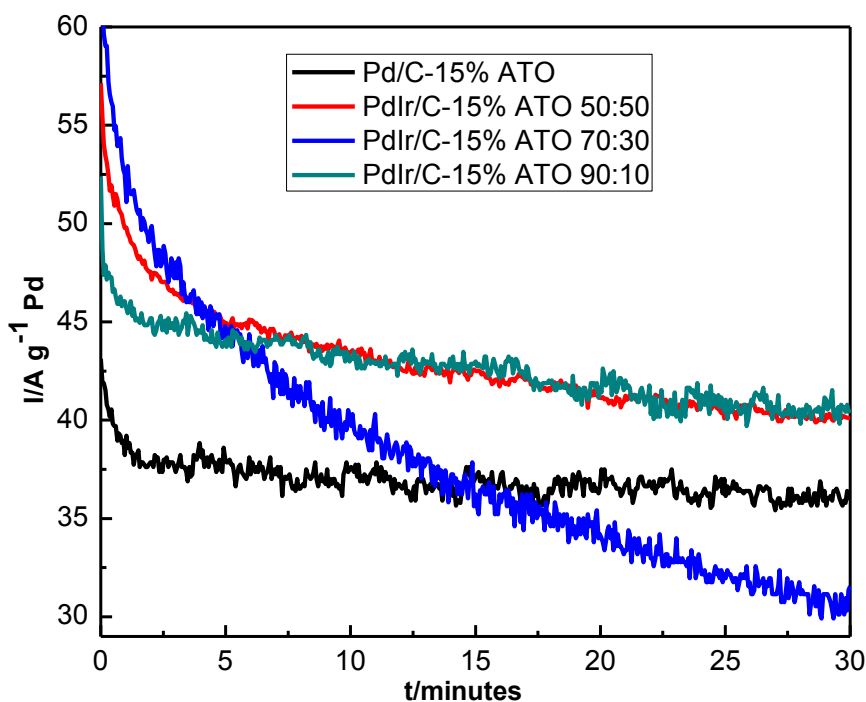


Figure 5. Current-time curves at 0.5 V in 1 mol L⁻¹ ethanol solution in 0.5 mol L⁻¹ H₂SO₄ for Pd/C-Sb₂O₅.SnO₂ and PdIr/C-Sb₂O₅.SnO₂ electrocatalysts at 25°C.

The final current values at 0.5 V (T = 25°C) increase in the following order: PdIr/C-Sb₂O₅.SnO₂ (50:50) ≈ PdIr/C-Sb₂O₅.SnO₂ (90:10) > Pd/C-Sb₂O₅.SnO₂ > PdIr/C-Sb₂O₅.SnO₂ (70:30). The activity of PdIr/C-Sb₂O₅.SnO₂ (50:50) and PdIr/C-Sb₂O₅.SnO₂ (90:10) was higher than that of the Pd/C-Sb₂O₅.SnO₂ indicating that the activity and stability of Pd could be improved due to the co-presence of Ir. The electronic modification of Pd might be the possible reasons for the enhanced activity, as the proximity of Ir and Pd atoms on the surface of the C-Sb₂O₅.SnO₂ (mechanism bifunctional).

4. CONCLUSIONS

The borohydride reduction method was an efficient process to produce PdIr/C-Sb₂O₅.SnO₂ for formic acid electro-oxidation.

PdIr/C-Sb₂O₅.SnO₂ electrocatalysts showed a broad peak at about 25° associated with the Vulcan XC72 support, four peaks at approximately 2θ = 40°, 47°, 67° and 82°, which are associated with the fcc structure characteristic of Pd or Pd alloys and peaks at about 2θ = 27°, 34°, 38°, 52°, 55°, 62°, 65°, 66°, which were also characteristic of ATO used as support. PdIr/C-Sb₂O₅.SnO₂ also no showed peaks related to Ir, however the presence of Ir oxides in small amounts and amorphous forms cannot be discarded.

PdIr/C-Sb₂O₅.SnO₂ (50:50) exhibited superior performance for formic acid electro-oxidation in comparison with others electrocatalysts prepared. The highest catalytic activity of PdIr/C-Sb₂O₅.SnO₂ (50:50) seems to be related to the combination of the bifunctional mechanism and the electronic effect. Further work is now necessary to investigate the mechanism of formic acid electro-oxidation using these electrocatalysts.

ACKNOWLEDGMENTS

The authors thank the Laboratório de Microscopia do Centro de Ciências e Tecnologia de Materiais (CCTM) by TEM measurements, FAPESP (2011/18246-0, 2012/03516-5) and CNPQ (501342/2012-5, 150639/2013-9) for the financial support.

References

1. Z. Bai, H. Yan, F. Wang, L. Yang, K. Jiang, *Ionics*, 19 (2013) 543-548.
2. W.J. Zhou, B. Zhou, W.Z. Li, Z.H. Zhou, S.Q. Song, G.Q. Sun, Q. Xin, S. Douvartzides, M. Goula, P. Tsiakaras, *Journal of Power Sources*, 126 (2004) 16-22.
3. F. Kadirgan, S. Beyhan, T. Atilan, *International Journal of Hydrogen Energy*, 34 (2009) 4312-4320.
4. X. Yu, P.G. Pickup, *Journal of Power Sources*, 182 (2008) 124-132.
5. L. Feng, S. Yao, X. Zhao, L. Yan, C. Liu, W. Xing, *Journal of Power Sources*, 197 (2012) 38-43.
6. A.S. Bauskar, C.A. Rice, *Electrochimica Acta*, 93 (2013) 152-157.
7. H. An, H. Cui, D. Zhou, D. Tao, B. Li, J. Zhai, Q. Li, *Electrochimica Acta*, 92 (2013) 176-182.
8. X. Wang, Y. Tang, Y. Gao, T. Lu, *Journal of Power Sources*, 175 (2008) 784-788.
9. R.M. Piasentin, R.F.B.d. Souza, J.C.M. Silva, E.V. Spinacé, M.C. Santos, A.O. Neto, *Int J Electrochem Sc*, 8 (2013) 435-445.
10. A. Oliveira Neto, M. Brandalise, R.R. Dias, J.M.S. Ayoub, A.C. Silva, J.C. Penteado, M. Linardi, E.V. Spinacé, *International Journal of Hydrogen Energy*, 35 (2010) 9177-9181.
11. E.V. Spinacé, R. Dias, M. Brandalise, M. Linardi, A. Neto, *Ionics*, 16 (2010) 91-95.
12. M. Marinšek, M. Šala, B. Jančar, *Journal of Power Sources*, 235 (2013) 111-116.
13. W. Zhou, J.Y. Lee, *The Journal of Physical Chemistry C*, 112 (2008) 3789-3793.
14. J. Ribeiro, D.M. dos Anjos, K.B. Kokoh, C. Coutanceau, J.M. Léger, P. Olivi, A.R. de Andrade, G. Tremiliosi-Filho, *Electrochimica Acta*, 52 (2007) 6997-7006.
15. K. Juodkasis, J. Juodkazytė, T. Juodienė, V. Šukienė, I. Savickaja, *Electrochimica Acta*, 51 (2006) 6159-6164.